

Measurement of Radiated Power Loss on EAST

This article has been downloaded from IOPscience. Please scroll down to see the full text article.

2011 Plasma Sci. Technol. 13 546

(<http://iopscience.iop.org/1009-0630/13/5/07>)

View [the table of contents for this issue](#), or go to the [journal homepage](#) for more

Download details:

IP Address: 61.190.88.139

The article was downloaded on 21/10/2011 at 03:57

Please note that [terms and conditions apply](#).

Measurement of Radiated Power Loss on EAST*

DUAN Yanmin (段艳敏), HU Liqun (胡立群), MAO Songtao (毛松涛),
 XU Ping (许平), CHEN Kaiyun (陈开云), LIN Shiyao (林士耀),
 ZHONG Guoqiang (钟国强), ZHANG Jizong (张继宗), ZHANG Ling (张凌),
 WANG Liang (王亮)

Institute of Plasma Physics, Chinese Academy of Sciences, Hefei 230031, China

Abstract A type of silicon detector known as AXUV (absolute extreme ultraviolet) photodiodes is successfully used to measure the radiated power in EAST. The detector is characterized by compact structure, fast temporal response (<0.5 s) and flat spectral sensitivity in the range from ultra-violet to X-ray. Two 16-channel AXUV arrays are installed in EAST to view the whole poloidal cross-section of plasma. Based on the diagnostic system, typical radiation distributions for both limiter and divertor plasma are obtained and compared. As divertor detachment occurs, the radiation distribution in X-point region is observed to vary distinctly. The total radiation power losses in discharges with different plasma parameters are briefly analyzed.

Keywords: radiated power loss, AXUV photodiode, EAST

PACS: 52.70.Kz, 52.55.Fa, 07.20.Fw

1 Introduction

In tokamak plasma, part of the input power can be dissipated by radiation. Therefore, accurate measurement of radiated power is important for the study of power balance and heat transport. In the last decade, the absolute extreme ultraviolet (AXUV) photodiodes detector was developed and successfully applied in the measurement of the radiated power in many fusion devices [1~4]. These detectors nearly exhibit theoretical quantum efficiency down to very low photon energy and have a flat spectral response over a wide range of photon energy. Different with the standard metal foil resistive bolometer, the AXUV photodiode is insensitive to low energy neutral particle ($E_{\text{particle}} < 500$ eV) and to microwave radiation from the electron cyclotron heating system. Furthermore, fast response and compact structure make it easier to achieve high temporal and spatial measurement in fusion experiments.

EAST is a superconducting tokamak with non-circular cross-section and mainly devoted to the study of physical issues related to the steady-state advanced operational modes for the future devices. The main parameters for EAST are the toroidal magnetic field of up to 3.5 T, the plasma current of up to 1 MA [5], the major radius R of 1.7 m to 1.9 m, the minor radius a of 0.4 m to 0.45 m and the elongation κ of 1.2 to 1.9. Configurations of single-null (SN) divertor, double-null (DN) divertor and elongated limiter configuration can be achieved. Up to now, the lower hybrid current drive (LHCD) system with a power of 2 MW at a frequency of 2.45 GHz [6] and the ion cyclotron resonance heating (ICRF) system including three generators with a power of 1.5 MW for each in a frequency range from 25 MHz

to 70 MHz are equipped. More than thirty diagnostics are installed to measure the elementary plasma parameters [7~10]. Two fast bolometry cameras based on AXUV detectors were built up to measure the radiated power from plasma.

In this paper, the AXUV diagnostic system is described in section 2 and some experimental results are given in section 3. Finally, summary and future plan are briefly presented in section 4.

2 Experimental setup

Two AXUV cameras, each with sixteen channels, were installed in EAST at the same toroidal location, as shown in Fig. 1. The two arrays were designed to fully cover the poloidal cross-section of plasma with a spatial resolution δr of about 4.5 cm. In front of the line array, an aperture of 1 mm \times 5 mm was used to confine the photon intensity. The distance between the detectors and the aperture are 66 mm. This geometrical arrangement determined an etendue of about 1×10^8 m² · sr without any overlap between channels. For a total radiated power of 1 MW, the output current of the detector was about 10 μ A and transmitted directly into amplifiers by an in-vessel twisted cable of 1.5 m, 32-pin feedthrough and an out-vessel twisted cable of 10 m. The amplifiers first convert the weak current signals to voltage signals and then amplify them. The gains of amplifiers are optional among 1×10^5 , 5×10^5 and 1×10^6 . Finally, the output voltage signals of amplifiers are connected to the common interface of data acquisition system. The AXUV detector can reach a time response below 1 μ s and the sampling frequency is 100 kHz in EAST.

*supported by National Natural Science Foundation of China (No.10935004) and National Magnetic Confinement Fusion Science Program of China (Nos. 2010GB106000, 2010GB106004)

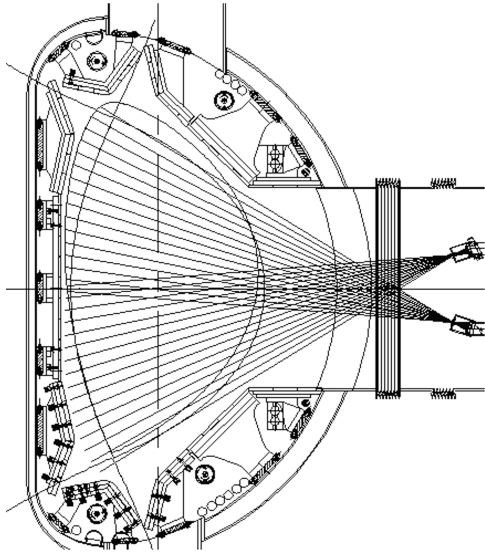


Fig.1 Geometry of viewing chords for the AXUV arrays in EAST

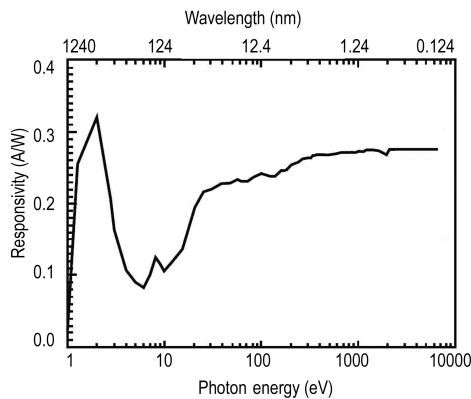


Fig.2 Theoretical response of AXUV photodiode detector

The AXUV detector is AXUV-16ELG linear array of 16 $p-n$ junction photodiodes (IRD Corp., USA) [11]. The sensitive area per channel is $2 \times 5 \text{ mm}^2$ and the spacing between two channels is 0.12 mm. Fig. 2 shows the spectral response of the AXUV detector. The responsivity has a theoretical value of about $0.26 \text{ A/W} \pm 5\%$ for the photons from 0.2 keV to 6 keV and will decrease sharply for photons energy below 20 eV. The lower sensitivity in the region 5 eV to 20 eV is mainly caused by the quantum efficiency loss due to the front passivating layer (SiO_2) absorption and reflection. In addition, the calculated sensitivity value at low photon energy is also affected by the varied average energy needed to generate one electron-hole pair which is a constant of about 3.65 eV at high energy. For photon energy above 6 keV, the sensitivity reduces quickly because the absorption length of photon exceeds the effective silicon thickness. For one linear array, the variation between channels is negligible quoted by IRD Cop., therefore calibration is unnecessary. For one experimental campaign of about 4000 shots in EAST, the sensitivity of a new detector might not be decreased

by the radiation damage, so the sensitivity for different channels is considered to be the same in analyzing data.

3 Measurement results

Typical profiles of radiated power in both limiter and divertor discharge are shown in Fig. 3, where the ordinate is the radiated power brightness (chord-integrated intensity of emissivity) in W/m^2 and the abscissa is the chord position in geometrical coordinate system. Fig. 3(a) and (b) are, respectively, the radiated power profile at 3.2 s for shots #28600 and #28427 with the same plasma current of 300 kA. Shot #28600 is Ohmic limiter plasma with a line-averaged density of $2.1 \times 10^{19} \text{ m}^{-3}$, while shot #28427 is Ohmic DN divertor plasma with a line-averaged density of $1.0 \times 10^{19} \text{ m}^{-3}$. Two profiles in Fig. 3 clearly indicate that the intense radiation comes mainly from core plasma for limiter plasma, while the radiation distribution in bulk plasma gets more flat with the enhancing radiation in the X-point region for divertor plasma. It is also found that the radiation in the X-point region exhibited higher peak which exceeded distinctly the intensity of core plasma when the plasma was in a detached operational mode. A temporal evolution of a typical detachment shot in density ramp-up phase is shown in Fig. 4. This shot is Ohmic DN divertor plasma with $I_p = 250 \text{ kA}$. Detachment is achieved by slowly ramping up the plasma density via puffing of deuterium, the working gas. It is found in Fig. 4 that the ion saturation current I_s starts to decrease at 4.2 s after a rollover phase as the density increases further which marks the beginning of the detachment phase [12,13]. At the same time, the radiated power in the X-point region increases quickly at 4.2 s while the increase in radiated power in the core plasma is rather weak. The intense radiation in the X-point region probably comes from line emission of low-charged impurity, such as CIII and D_α which are also found increasing in quantity. The profiles of radiated power and visible CIII radiation at different time are shown in Fig. 5, for the same shot as in Fig. 4. It is shown that the radiated power dominates near the X-point region and then shift to core plasma after detachment. The radiation peak of visible CIII is also found shifting towards the X-point first and then back to the outer target region after detachment. This phenomenon is similar to previous observation in other tokamaks [14,15]. Owing to absence of enough viewing chords in divertor region at present, clearer image showing the radiation variation during the detachment process is anticipated in future study.

The total radiated power can be calculated from the following equation:

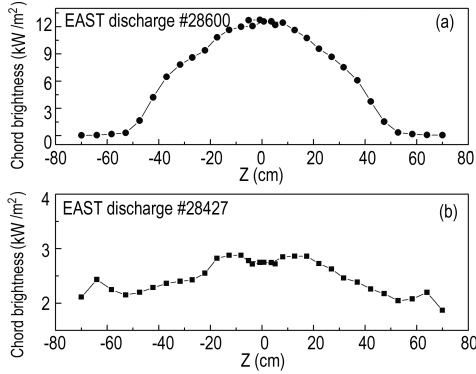
$$P_{\text{rad}} = \sum_i 2\pi R_i \Delta r_i P_i. \quad (1)$$

Here R_i is the major radius of the center of viewing chord, Δr_i is the averaged width between the i^{th} viewing chord and the $(i+1)^{\text{th}}$ viewing chord, and P_i is the

radiated power integrated along the i^{th} chord, which can be calculated by

$$P_i = \frac{4\pi l^2}{A_d A_a \cos \theta \cos \theta'} P_d, \quad (2)$$

where, P_d is the radiated power received by the i^{th} detector, A_d and A_a are the areas of detector and aperture, θ and θ' are the viewing chord angle from the normal of detector and the normal of aperture, respectively, and l is the distance from the detector to the aperture. The overlap of chords between two arrays is subtracted.



(a) For limiter circular cross-section of shot #28800 at 3.2 s, (b) For DN divertor configuration of shot #28427 at 3.2 s
Fig.3 Profiles of typical chord brightness from AXUV array

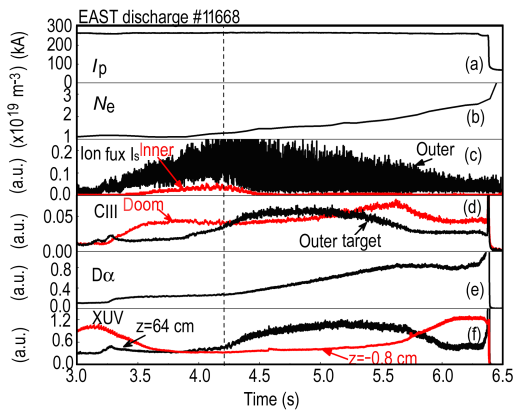
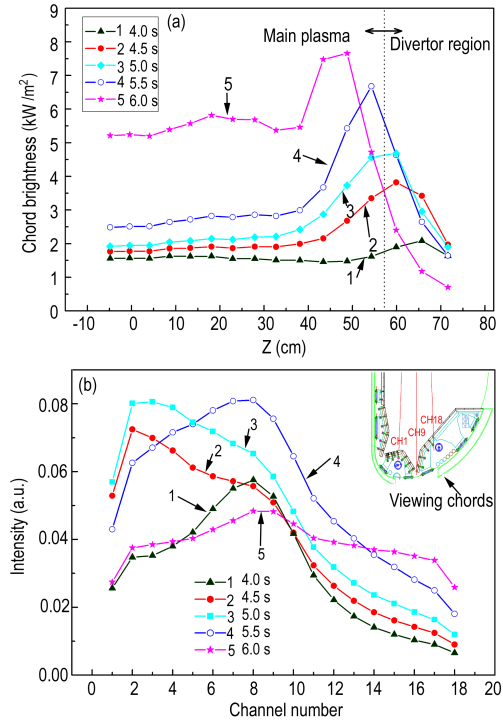


Fig.4 Temporal evolution of a typical detachment discharge in density ramp-up phase. The data shown from up to bottom are: (a) Plasma current I_p , (b) Central line-averaged electron density N_e , (c) Ion saturation current I_s , measured by Langmuir probes embedded in divertor target plates, (d) Intensity of visible CIII emission, (e) Intensity of D_α emission near X-points, (f) Intensity of radiated power, measured by AXUV photodiodes. The dashed line corresponds to the beginning of plasma detachment

In general, the total radiated power increases with the electron density and the plasma current. It is about 25% to 40% of input heating power in limiter Ohmic plasma. In LHW heating experiments, it is found that the total radiated power increases with the increase in

power of LHW. In divertor plasma, the total radiated power obtained from the AXUV arrays will underestimate the real radiated power loss. One main reason is the incomplete coverage of viewing chords on the divertor region and the other reason is that the sensitivity the AXUV sensor is reduced in the energy range of 5 eV to 15 eV where the line emission of low-charged impurities (CIII, D_α) is strong at plasma edge.



(a) Profiles of radiated power from the AXUV photodiodes, (b) Profiles of visible CIII emission in divertor region
Fig.5 Comparison of profiles at 4.0 s, 4.5 s, 5.0 s, 5.5 s and 6.0 s for the shot shown in Fig. 4

4 Summary and future plan

The AXUV photodiode detectors are used as fast bolometry in EAST. Two horizontal arrays to cover the whole poloidal cross-section of plasma work well. For limiter plasma with a circular cross-section, the radiation profiles are normal symmetrical. For divertor plasma, the radiation profiles become flat with the increase in radiation intensity in divertor region. For detached plasma, a marked radiation increase in the X-point region and a shift of radiation center can be observed. Based on the present viewing chords, the total radiated power loss is calculated for EAST with different plasma parameters. In limiter plasma, the fraction of radiated power loss is no more than 40%.

Tomographic reconstruction of local emissivity from line-integrated measurements is highly necessary for studying particle transports. For circular cross-section of plasma, Abel inversion is used for one dimensional reconstruction based on the present-XUV arrays. However, the radiated power distribution for divertor

plasma is usually complicated, especially in the divertor region and boundary. A reliable two dimensional reconstruction of the radiation emissivity needs more viewing chords to cover the poloidal cross-section from different directions [3,16,17]. Another two AXUV photodiodes arrays in vertical direction are being designed and will be installed in one upper port in the next EAST experimental campaign. The vertical arrays adopt a plug-in supporting structure with an active water cooling system, which can make the detector work below 30°C, even in a baking environment of 300°C. In addition, a 48 channels metal resistor bolometers using Pt absorber were tested and will work normally in near future.

Acknowledgements

It is a pleasure to acknowledge the assistance of EAST team to this work.

References

- 1 Boivin R L, Goetz J A, Marmar E S, et al. 1999, Rev. Sci. Instrum., 70: 260
- 2 Maqueda R J, Wurden G A, Crawford E A. 1992, Rev. Sci. Instrum., 63: 4717
- 3 Liu Y, Kostrioukov A Yu, Peterson B J, et al. 2003, Rev. Sci. Instrum., 74: 4717

- 4 Furno I, Weisen H, Mlynar J, et al. 1999, Rev. Sci. Instrum., 70: 4552
- 5 Wan Y X, HT-7 Team, HT-7U Team. 2000, Nucl. Fusion, 40: 1057
- 6 Zhao L M, Shan J F, Liu F K, et al. 2010, Plasma Sci. Technol., 12: 118
- 7 Xu P, Lin S Y, Hu L Q, et al. 2010, Rev. Sci. Instrum., 81: 063501
- 8 Shi Y J, Wang F D, Wan B N, et al. 2010, Plasma Phys. Control. Fusion, 52: 085014
- 9 Yang L, Wan B N, Zhao J Y, et al. 2010, Plasma Sci. Technol., 12: 284
- 10 Gao X. 2008, Instrum. Exp. Tech., 51: 246
- 11 <http://www.ird-inc.com>
- 12 Guo H Y, Gao X, Li J, et al. 2010, J. Nucl. Mater., doi:10.1016/j.jnucmat.2010.11.048
- 13 Loarte A, Monk R D, Martín-solís J R, et al. 1998, Nucl. Fusion, 38: 331
- 14 Fenstermacher M E, Wood R D, Allen S L, et al. 1997, J. Nucl. Mater., 241~243: 666
- 15 Kubo H, Ishida S, Sakasai A, et al. 1993, Nucl. Fusion, 33: 1427
- 16 Reinke M L, Hutchinson I H. 2008, Rev. Sci. Instrum., 79: 10F306
- 17 Konoshima S, Leonard A W, Ishijima T, et al. 2001, Plasma Phys. Control. Fusion, 43: 959

(Manuscript received 24 February 2011)

(Manuscript accepted 23 August 2011)

E-mail address of DUAN Yanmin: ymduan@ipp.ac.cn